RESEARCH ARTICLE

NANO · MICRO small
www.small-journal.com

Orthogonal Design of Experiments for Engineering of Lipid Nanoparticles for mRNA Delivery to the Placenta

*Hannah C. Safford, Kelsey L. Swingle, Hannah C. Geisler, Alex G. Hamilton, Ajay S. Thatte, Aditi A. Ghalsasi, Margaret M. Billingsley, Mohamad-Gabriel Alameh, Drew Weissman, and Michael J. Mitchell**

During healthy pregnancy, the placenta develops to allow for exchange of nutrients and oxygen between the mother and the fetus. However, placental dysregulation can lead to several pregnancy disorders, such as preeclampsia and fetal growth restriction. Recently, lipid nanoparticle (LNP)-mediated delivery of messenger RNA (mRNA) has been explored as a promising approach to treat these disorders. Here, iterative libraries of LNPs with varied excipient molar ratios are screened in vitro for enhanced mRNA delivery to placental cells with minimal cytotoxicity when compared to an LNP formulation with a standard excipient molar ratio. LNP C5, the top formulation identified by these screens, demonstrates a fourfold increase in mRNA delivery in vitro compared to the standard formulation. Intravenous administration of LNP C5 to pregnant mice achieves improved in vivo placental mRNA delivery compared to the standard formulation and mediates mRNA delivery to placental trophoblasts, endothelial cells, and immune cells. These results identify LNP C5 as a promising optimized LNP formulation for placental mRNA delivery and further validates the design of experiments strategy for LNP excipient optimization to enhance mRNA delivery to cell types and organs of interest.

1. Introduction

Ionizable lipid nanoparticles (LNPs) have recently emerged as the most clinically advanced non-viral platform for therapeutic delivery of nucleic acids. The use of LNPs to deliver messenger RNA (mRNA) holds great therapeutic promise to enable transient protein expression without the risks associated with genomic integration, minimizing off-target effects.[1–3] LNPs are advantageous delivery vehicles due to their highly modular nature, strong biocompatibility, and ability to enable potent intracellular mRNA delivery.[1,2,4–10] Additionally, LNPs can overcome many of the challenges otherwise associated with in vivo mRNA delivery, including rapid degradation and poor cellular uptake due to its negative charge and large size.[1,2] Given these advantages, LNP-mediated mRNA delivery has been applied to a wide range of therapeutic applications, including protein

H. C. Safford, K. L. Swingle, H. C. Geisler, A. G. Hamilton, A. S. Thatte, A. A. Ghalsasi, M. M. Billingsley, M. J. Mitchell
Department of Bioengineering
University of Pennsylvania
Philadelphia, PA 19104, USA
E-mail: mjmitch@seas.upenn.edu

M.-G. Alameh, D. Weissman
Department of Medicine
University of Pennsylvania
Philadelphia, PA 19104, USA

M.-G. Alameh, D. Weissman, M. J. Mitchell
Penn Institute for RNA Innovation
Perelman School of Medicine
University of Pennsylvania
Philadelphia, PA 19104, USA

M. J. Mitchell
Abramson Cancer Center
Perelman School of Medicine
University of Pennsylvania
Philadelphia, PA 19104, USA

M. J. Mitchell
Institute for Immunology
Perelman School of Medicine
University of Pennsylvania
Philadelphia, PA 19104, USA

M. J. Mitchell
Cardiovascular Institute
Perelman School of Medicine
University of Pennsylvania
Philadelphia, PA 19014, USA

M. J. Mitchell
Institute for Regenerative Medicine
Perelman School of Medicine
University of Pennsylvania
Philadelphia, PA 19104, USA

The ORCID identification number(s) for the author(s) of this article can be found under https://doi.org/10.1002/smll.202303568

DOI: 10.1002/smll.202303568

replacement therapy, cancer immunotherapy, gene editing and, most notably, the recent success of the COVID-19 vaccines.[2–4,7–9,11–14]

Recently, LNPs have been explored for therapeutic applications during pregnancy, specifically for mRNA delivery to the placenta.[15–17] The placenta is an organ that develops throughout pregnancy to support fetal development. Its primary role is to serve as a biological barrier between maternal and fetal circulation, protecting the fetus from any harmful molecules and providing a site for nutrient and oxygen exchange.[18–20] Placental disorders, such as preeclampsia and fetal growth restriction, can arise during pregnancy as a result of dysfunctional placental development and can lead to immediate and long-term complications for both mother and fetus.[21,22] It is estimated that 4 million women are diagnosed with preeclampsia each year, and fetal growth restriction is the greatest risk factor for still birth; both disorders are leading causes of maternal and fetal morbidity and mortality worldwide.[21–23]

Despite the global prevalence of preeclampsia and fetal growth restriction, treatment options are severely lacking. Management of these disorders usually relies on early delivery of the fetus and placenta to prevent severe complications of each disease.[21,22,24,25] Given the lack of available therapeutics, researchers have focused on replacing growth factors found to be deficient in these conditions as a possible solution. Prior studies have investigated the use of LNPs to deliver mRNA encoding either vascular endothelial growth factor (VEGF) or placental growth factor (PlGF) to the placenta.[15,16] It is thought that through overexpression of these vital proteins, normal placental function can be restored.

To effectively design LNPs that can deliver mRNA to the placenta, it is important to understand the structures, cell types and barriers present at the placental interface. Mouse models have been essential to investigate new therapeutics for use during pregnancy. Mice are commonly used as there are several integral placental features that are shared between mouse placentas and human placentas. Specifically, trophoblasts are the main cell type present in the placentas of both species.[26,27]

The structure of the mouse placenta can be divided into three separate regions: the decidua, the junctional zone and the labyrinth (**Figure 1**A, left). The decidua is the region that lies closest to the maternal side and functions as a mucosal layer that regulates trophoblast invasion to ensure proper embryo implantation and placental development. Additionally, it is home to many of the immune cells that reside in the placental environment. The region bordering the decidua is the junctional zone, which serves as the main endocrine compartment of the placenta. The decidua and junctional zone are separated by a layer of trophoblast giant cells (TGCs), which are also involved in supporting embryo implantation into the uterus. Lastly, the final region of the placenta is the labyrinth, the primary site of nutrient and gas exchange between the mother and the fetus.[26,27] The exchange interface of the placental labyrinth is composed of two syncytiotrophoblast layers and a layer of fetal endothelial cells (Figure 1A, right). TGCs are also present as this interface but do not form a continuous barrier.[26] Endothelial cells, immune cells and trophoblast cells, specifically the syncytiotrophoblast layer, secrete proteins into the placental environment, and as such are target cells of interest for LNP-mediated mRNA delivery in the placenta.[28–30]

To maximize mRNA delivery to an organ or cell type of interest, such as the placenta, the excipient molar ratios of an LNP formulation can be optimized.[4–6,9,16,31–32] LNPs are typically formulated as four component systems where the main excipients used are an ionizable lipid, phospholipid, cholesterol, and lipid-anchored poly(ethylene glycol) (PEG). Each excipient plays an important role in promoting LNP-mediated delivery of mRNA (Figure 1B).[2,3,11,34] Ionizable lipids are an important component of LNPs as they become positively charged in acidic environments.[3,4,34] This shift in charge improves cargo encapsulation efficiency by complexing with the negatively charged mRNA during formulation. This charge shift additionally aids in endosomal escape of LNPs through membrane disruption.[3,4,15,34] Cholesterol plays an important structural role by modulating membrane rigidity to enhance LNP stability.[2,4] The inclusion of the phospholipid 1,2-dioleoyl-*sn*-glycero-3-phosphoethanolamine (DOPE) can also improve endosomal escape through destabilization of endosomal membranes as well as support LNP stability.[3,4,9,34,35] Lastly, the lipid-anchored PEG reduces aggregation, protein absorption, and immune cell recognition of LNPs while also enhancing circulation time.[2–4,11,34] Modulation of these distinct LNP excipient components and their molar ratios can lead to changes in the physicochemical properties of the LNPs, including their size, shape, surface properties, morphology and stability, ultimately impacting LNP efficacy and uptake into different cell types.[3–5,7,33,34,36] As LNP delivery to the placenta is still in its infancy, optimization of excipients is vital to improving LNP-mediated mRNA delivery to the placenta.

Recent work published by our lab screened a library of LNPs formulated with 15 novel ionizable lipids for mRNA delivery to trophoblasts. Following systemic administration in pregnant mice, LNPs formulated with our lead ionizable lipid C12-494 were able to more potently deliver mRNA to the placenta compared to LNPs formulated with an industry standard ionizable lipid, C12-200.[15] However, these LNPs were formulated using a standard excipient molar ratio that was previously optimized for mRNA delivery to the liver.[5] Here, we used the principles of orthogonal design of experiments (DOE) to create sequential libraries of C12-494 LNPs with varied excipient molar ratios to identify lead formulations for enhanced in vivo mRNA delivery to the placenta (Figure 1C). Utilizing four molar ratios each of C12-494, DOPE, cholesterol and lipid-anchored PEG, we engineered a design space of 256 possible LNP formulations which we evaluated using a library of 16 representative LNP formulations, termed library A. We screened library A in BeWo b30 cells, a human trophoblast cell line, to assess mRNA delivery and cytotoxicity in comparison to the standard excipient formulation, LNP S1. Trends in mRNA delivery based on excipient molar ratios were used to design two sequential libraries, B and C, within a narrowed range of excipient molar ratios. Libraries B and C were again screened in BeWo b30 cells to identify individual formulations with potent mRNA delivery and minimal cytotoxicity when compared to LNP S1. Finally, the top two formulations across all libraries were screened for in vivo luciferase mRNA delivery to murine placentas. LNP C5 was identified as the lead formulation, demonstrating potent mRNA delivery to the placenta as well as reduced mRNA delivery to the maternal liver. Finally, LNP C5 demonstrated the ability to mediate

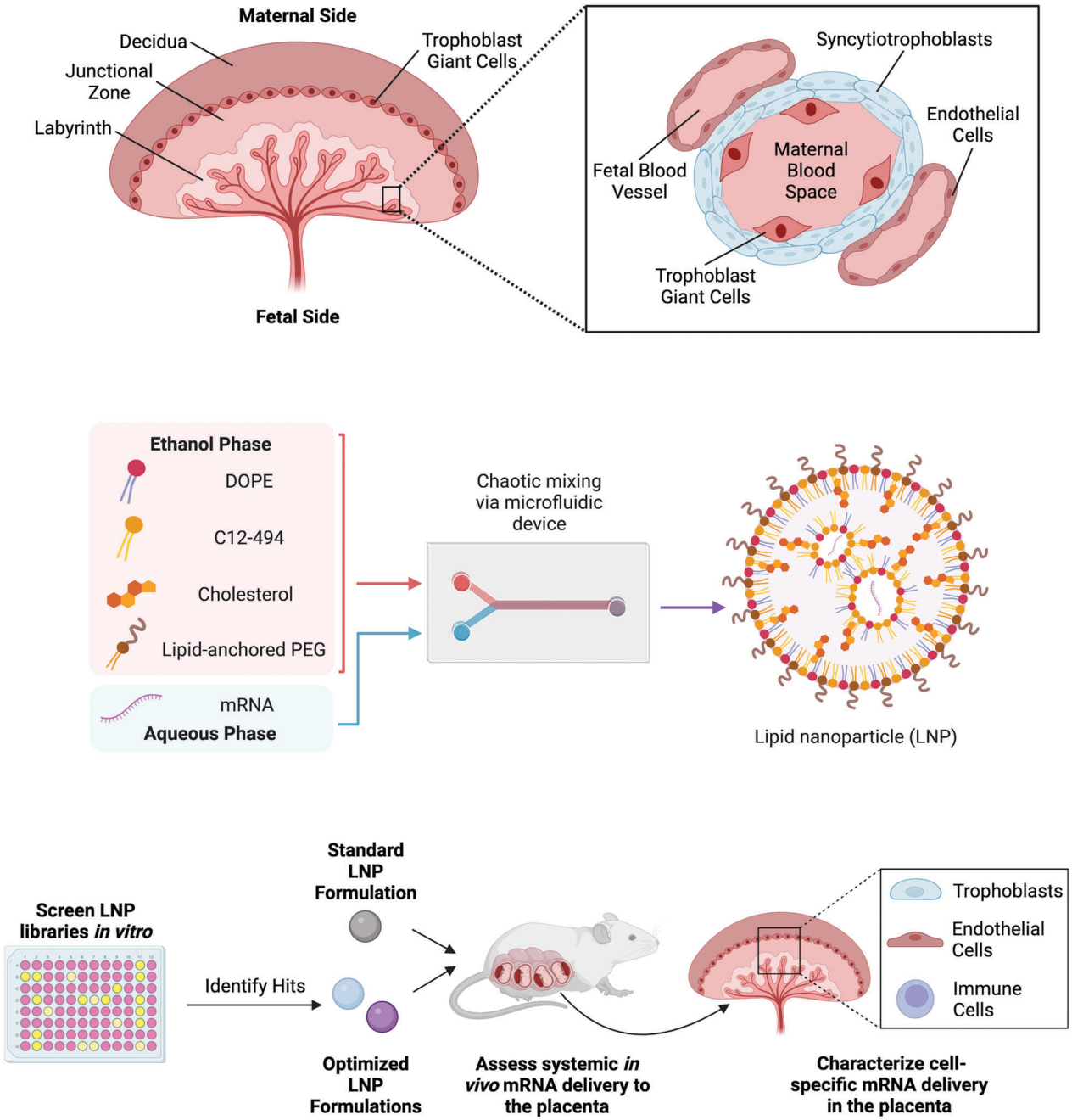

Figure 1. A) Left: structure of the mature mouse placenta which consists of three regions: the decidua, the junctional zone and the labyrinth. Right: zoomed in view of the labyrinth region and the cell types that separate maternal circulation from fetal circulation. Redrawn from ref. [15]. B) Schematic of LNP synthesis where an ethanol phase, containing DOPE, the ionizable lipid C12-494, cholesterol and lipid-anchored PEG, was mixed with an aqueous phase, containing mRNA, in a microfluidic device to formulate LNPs. C) Schematic of experimental design where LNP libraries were screened in vitro to identify high-performing LNP formulations which were further evaluated in vivo for LNP-mediated mRNA delivery to the placenta in pregnant mice.

mCherry expression in trophoblasts, endothelial cells and immune cells in the placenta. Taken together, these results confirm the potential of LNP C5 to potently deliver mRNA to the placenta and support the importance of optimizing LNP excipient molar ratios to improve mRNA delivery to an organ or cell type of interest.

2. Results and Discussion

2.1. Formulation and Characterization of Library A LNPs

Previous work has reported optimized LNP excipient molar ratios for mRNA delivery to the liver; trends indicated that decreased

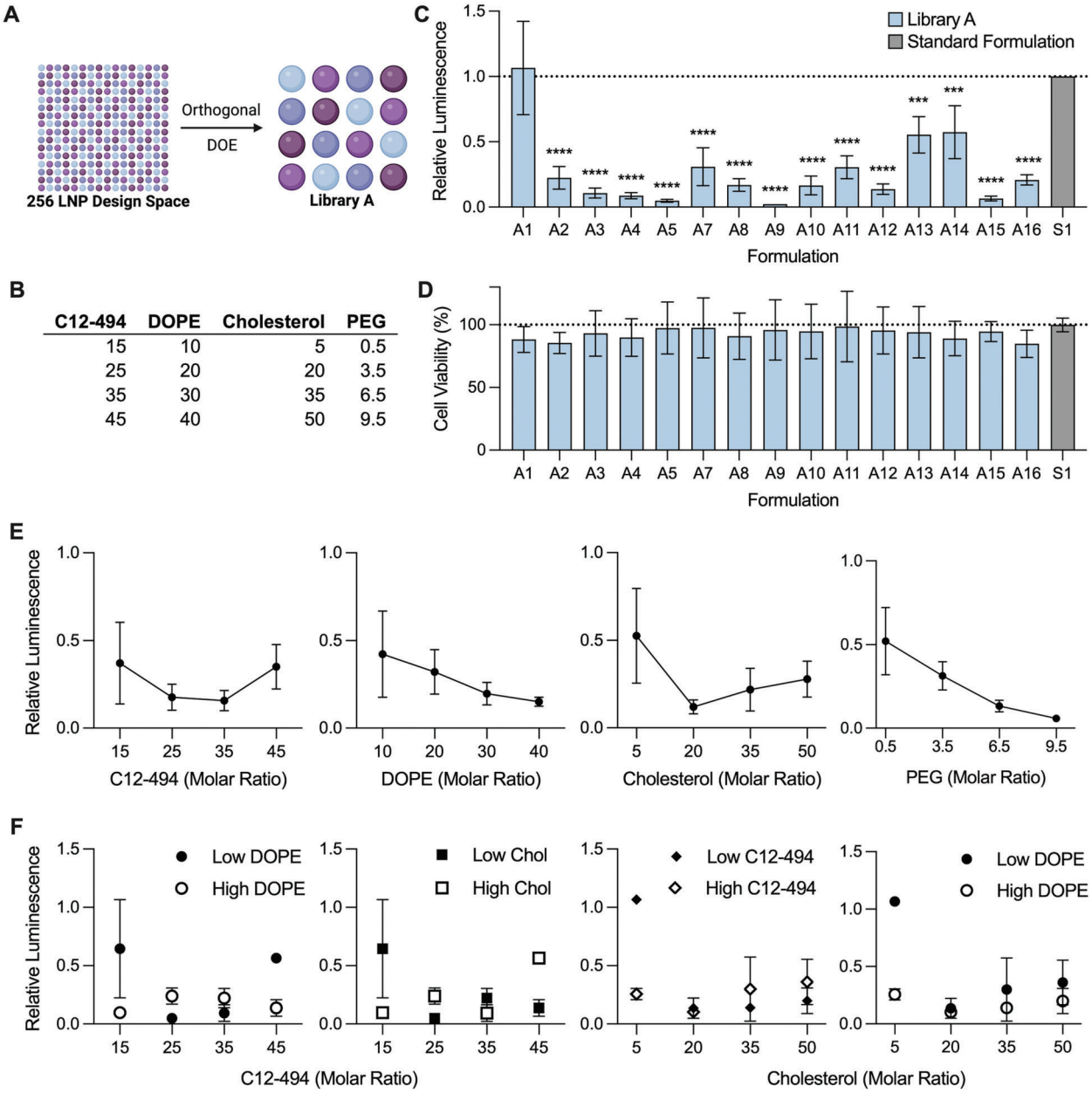

Figure 2. In vitro screening of library A for LNP-mediated luciferase mRNA delivery to BeWo b30 trophoblast cells. A) Schematic of the orthogonal DOE process used to engineer library A with 16 representative LNP formulations. B) Levels of excipient molar ratios used to generate library A. C) Luciferase expression and D) cell viability of BeWo b30 cells 24 h after treatment with library A LNPs or the standard formulation (S1) at a dose of 50 ng of luciferase mRNA per 50 000 cells. Relative luminescence was quantified by normalizing to cells treated with LNP S1 (dashed line in (C)) and cell viability was measured by normalizing to untreated cells (dashed line in (D)). Results are reported as mean ± standard deviation from $n = 3$ biological replicates. Nested one-way ANOVAs with post hoc Student's t tests using the Holm–Šídák correction for multiple comparisons were used to compare the luciferase expression or cell viability across treatment groups to LNP S1, ***$p \leq 0.001$, ****$p \leq 0.0001$. E) Average luminescence values of the 4 LNP formulations at each molar ratio of C12-494, DOPE, cholesterol and PEG. Error bars = standard error of the mean. F) Average luminescence values of the 2 LNP formulations at a specific molar ratio of one excipient (C12-494 or cholesterol) and either the lower or higher molar ratios of the second excipient (DOPE, cholesterol or C12-494). Error bars = standard error of the mean.

ionizable lipid content and increased phospholipid, cholesterol, and PEG content led to improved mRNA delivery.[5] However, these parameters have not yet been optimized for mRNA LNP delivery to the placenta. Thus, an initial library of LNPs was engineered using orthogonal DOE where each of the four excipients was evaluated at four molar ratios using a library of 16 representative formulations (**Figure 2**A, Tables S1 and S2, Supporting Information). The initial molar ratios were selected based on previous investigations into excipient optimization.[5,6,30,31] Specifically, C12-494 was varied between 15% and 45%, DOPE between

10% and 40%, cholesterol between 5% and 50%, and PEG between 0.5% and 9.5% (Figure 2B). Throughout experimentation, the optimized LNPs for placental mRNA delivery were compared to the standard excipient mRNA formulation, LNP S1, which is formulated at a molar composition of 35% ionizable lipid:16% DOPE:46.5% cholesterol:2.5% PEG.[5]

To formulate the LNPs evaluated in this study, the ionizable lipid C12-494 was synthesized (Figure S1, Supporting Information) and combined with DOPE, cholesterol and lipid-anchored PEG in ethanol. This ethanol phase was then chaotically mixed with an aqueous phase containing mRNA in a microfluidic device to formulate each LNP (Figure 1B). After formulation, library A was characterized for size, zeta potential, mRNA concentration, and mRNA encapsulation efficiencies (Table S3, Supporting Information). The *z*-average size of the LNPs in library A ranged from 63.7 to 133.2 nm where 15 of the 16 LNP formulations had a polydispersity index (PDI) under 0.3, indicating uniform LNP formulation. The surface charge of the LNPs in library A remained neutral, between −5 and 5 mV, with the exception of LNP A14 which had a zeta potential of −18.1 mV. mRNA concentrations ranged from 23.5 to 45.7 ng μL^{-1} while mRNA encapsulation efficiencies varied from 0% to 85%. For many of the LNPs in library A, the size, PDI, surface charge, mRNA concentration and encapsulation efficiencies were comparable to that of the standard LNP formulation, S1.

2.2. Evaluation of Library A for In Vitro mRNA LNP Delivery to Trophoblasts

For in vitro screening, luciferase mRNA was encapsulated into LNPs as a reporter mRNA cargo, where luminescence signal from LNP-treated wells correlates to functional mRNA delivery. In vitro library screening was performed in BeWo b30 trophoblast cells, a human choriocarcinoma cells line. BeWo b30 cells were selected for library screening as they have been previously used to model the placental barrier and express several key placental differentiation markers, such as human chorionic gonadotrophin (hCG).[37–40] Additionally, several studies have used BeWo b30 cells to evaluate nanoparticle uptake in the placenta.[16,17,38]

To assess mRNA delivery to trophoblasts, BeWo b30 cells were treated with LNPs from library A and LNP S1 at a dose of 50 ng of luciferase mRNA per 50 000 cells. However, since LNP A6 exhibited 0% encapsulation efficiency, it was removed from the library screen. The 0% encapsulation efficiency exhibited by LNP A6 is likely due its molar composition, as it has considerably less cholesterol content and higher PEG content than the standard LNP formulation (Table S2, Supporting Information). 24 h after treatment, luciferase expression and cell viability were measured for all treatment groups and compared to the S1 formulation. All of the LNP formulations in library A, except for LNP A1, displayed significantly reduced mRNA delivery compared to LNP S1. LNP A1 was the only LNP formulation that achieved comparable mRNA delivery to trophoblasts compared to LNP S1 (Figure 2C). The reduced mRNA delivery observed for the LNP formulations in library A compared to LNP S1 is likely due to the wide range of excipient molar ratios evaluated in this initial library, where the molar compositions of the LNP formulations were too varied to demonstrate any significant improvement in mRNA delivery over the standard formulation. Additionally, none of the LNPs in library A nor LNP S1 caused cytotoxicity in the BeWo b30 cells 24 h after LNP treatment (Figure 2D).

While none of the formulations in library A enhanced mRNA delivery over the S1 formulation, the relationship between the different excipient molar ratios and mRNA delivery were investigated to identify trends that lead to improved mRNA delivery. To study these relationships, the average luminescence signal for all LNPs with the same molar ratio of a specific excipient were plotted (Figure 2E). This revealed that LNPs at both the lowest and highest ratios of C12-494 and LNPs at the lowest ratio of cholesterol led to the highest luminescence signal. Additionally, LNPs with decreased ratios of DOPE and PEG led to improved mRNA delivery to BeWo b30 cells. While the inclusion of DOPE into LNP formulations has been shown to improve mRNA delivery compared to other phospholipids, DOPE is also known to have an affinity toward liver cells, which perhaps elucidates why reduced DOPE content leads to improved mRNA delivery to BeWo b30 cells.[5,41,42] Furthermore, enhanced placental mRNA delivery with decreasing molar ratios of PEG may be explained by the need to balance the amount of PEG in LNP formulations to promote LNP stability without hindering cellular uptake of LNPs.[43–45]

Given these trends, we were interested in designing two subsequent libraries, one with low molar ratios of C12-494 and one with high molar ratios. To further inform our library design, we investigated the impact of excipient interactions on trends in mRNA delivery. To this end, we plotted the average luminescence signal from LNPs with the same molar ratio of one excipient with either the two lower or higher molar ratios of a second excipient (Figure 2F and Figure S2, Supporting Information). These relationships revealed that at both low and high ratios of C12-494, mRNA delivery was improved with lower amounts of DOPE and PEG. However, at low ratios of C12-494, mRNA delivery was improved with lower ratios of cholesterol while high ratios of C12-494 had improved delivery with higher ratios of cholesterol. Similarly, low ratios of cholesterol benefitted from lower ratios of C12-494 while high ratios of cholesterol had improved delivery with high ratios of C12-494. Additionally, mRNA delivery was improved with lower amounts of DOPE across all ratios of cholesterol. Interestingly, higher ratios of cholesterol saw improved delivery with higher amounts of PEG (Figure S2, Supporting Information).

These observed trends differ from prior work optimizing LNP formulations for a variety of different applications. Optimized LNP formulations for mRNA delivery to the liver saw improvements with decreased molar ratios of ionizable lipid and increased molar ratios of phospholipid, cholesterol and lipid-anchored PEG.[5] For applications in mRNA delivery to T cells, enhanced mRNA transfection was identified for LNP formulations with increased molar ratios of ionizable lipid and phospholipid and decreased molar ratios of cholesterol.[32] Lastly, optimization of the LNP formulation for new lipid-like materials observed improved mRNA delivery with decreased molar ratios of ionizable lipid, cholesterol, and lipid-anchored PEG and increased molar ratios of phospholipid.[6] The variability in the outcomes of LNP excipient optimization for different applications further supports the need to optimize LNP formulations for applications in placental mRNA delivery.

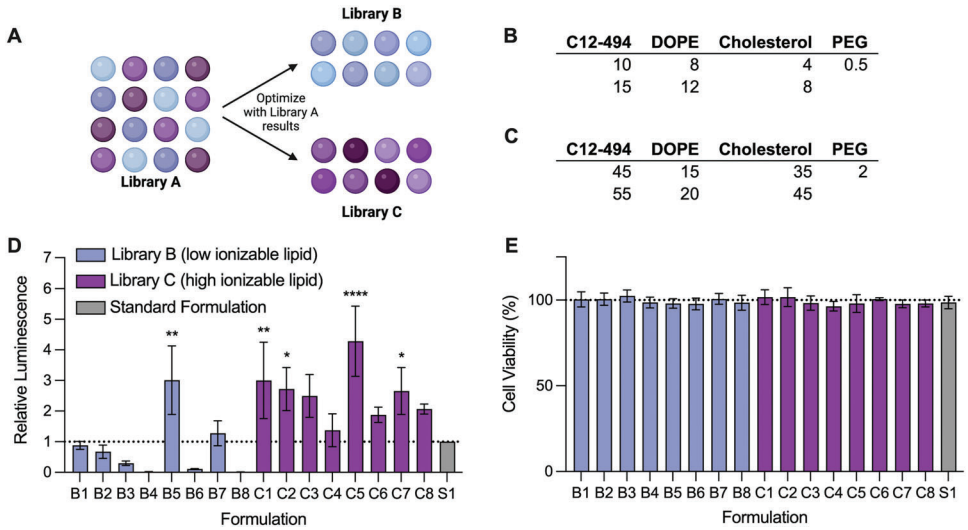

Figure 3. In vitro screening of libraries B and C for LNP-mediated luciferase mRNA delivery to trophoblast cells. A) Schematic of the orthogonal DOE process used to generate libraries B and C each containing 8 LNP formulations. Levels of excipient molar ratios used to generate B) library B or C) library C. D) Luciferase expression and E) cell viability of BeWo b30 cells 24 h after treatment with library B and C LNPs or LNP S1. Cells were treated with 50 ng of luciferase mRNA per 50 000 cells. Relative luminescence was quantified by normalizing to cells treated with LNP S1 (dashed line in (D)) and cell viability was measured by normalizing to untreated cells (dashed line in (E)). Results are reported as mean ± standard deviation from $n = 3$ biological replicates. Nested one-way ANOVAs with post hoc Student's t tests using the Holm–Šídák correction for multiple comparisons were used to compare the luciferase expression or cell viability across treatment groups to LNP S1, $*p \leq 0.05$, $**p \leq 0.01$, $****p \leq 0.0001$.

2.3. Further Optimization of LNP Excipients Enhances In Vitro mRNA LNP Delivery to Trophoblasts

Given the observed trends between excipient molar ratios and mRNA delivery, two sequential 8-LNP libraries were designed using DOE within a narrowed range of excipient molar ratios (**Figure 3**A). Library B was designed with lower molar ratios of C12-494, DOPE, cholesterol and a constant molar ratio of PEG while library C was designed with higher molar ratios of C12-494 and cholesterol, lower molar ratios of DOPE and again the PEG molar ratio was held constant (Figure 3B,C, Table S1 and S2, Supporting Information).

Both library B and C were characterized for size, zeta potential, mRNA concentration, and mRNA encapsulation efficiencies following formulation (Tables S4 and S5, Supporting Information). The LNPs in library B had a z-average size between 65.3 and 145.7 nm with PDIs less than 0.33. The zeta potential across the library varied from −5.89 to 3.03 mV. mRNA concentrations for LNPs in library B were measured between 11.6 and 39.2 ng μL^{-1} and encapsulation efficiencies were generally higher across library B compared to library A with 6 out of the 8 LNPs having encapsulation efficiencies greater than 80%. The LNPs in library C were larger in size than both library A and B, with z-average sizes ranging from 117.3 to 157.1 nm. PDIs across the library were less than 0.33 and the zeta potential for all LNP formulations was positive, varying from 1.28 to 6.88 mV. mRNA concentrations were measured between 28.67 and 34.67 ng μL^{-1} and average encapsulation efficiencies were higher than both library A and B, with all formulations having encapsulation efficiencies greater than 85%.

Both library B and C were screened in BeWo b30 cells to evaluate mRNA delivery and cytotoxicity in trophoblasts. Compared to LNP S1, library B contained one particle with significantly improved mRNA delivery, LNP B5, while all LNPs in library C had increased luciferase expression compared to LNP S1, with 4 LNPs demonstrating significantly higher mRNA delivery than the S1 formulation (Figure 3D). The top performing LNP in library C, LNP C5, exhibited a 4× increase in mRNA delivery compared to LNP S1 while the top performing LNPs in libraries B and A, LNP B5 and LNP A1, only exhibited a 3× improvement in or comparable mRNA delivery compared to LNP S1, respectively. Additionally, none of the LNPs in library B or C demonstrated any cytotoxicity in BeWo b30 cells (Figure 3E).

To confirm the results of the initial library screens, the top performing LNPs from each library, LNPs A1, B5, and C5, along with LNP S1 were further evaluated in a dose-dependent manner for in vitro luciferase expression and cell viability in BeWo b30 cells. Across all doses tested, LNP C5 demonstrated improved luciferase expression compared to LNP S1 (**Figure 4**A). At lower doses, LNPs A1 and B5 showed similar or slightly improved luciferase expression compared to LNP S1 while at the highest dose evaluated, both LNPs had significantly higher luciferase expression compared to LNP S1. Interestingly, while LNP A1 had comparable luciferase expression to LNP S1 across the lower doses, it exhibited the greatest improvement in luciferase expression at the highest dose. Additionally, none of the LNPs exhibited any cytotoxicity at the different doses that were tested (Figure 4B). Since LNP C5 exhibited the most consistent improvement in mRNA delivery across all doses, it was identified as the lead candidate for an optimized LNP formulation for trophoblast delivery and was selected for further evaluation in vivo. Additionally, given the strong improvement in mRNA delivery for LNP A1 at the highest dose, it was also selected for further evaluation in vivo for mRNA delivery to the placenta.

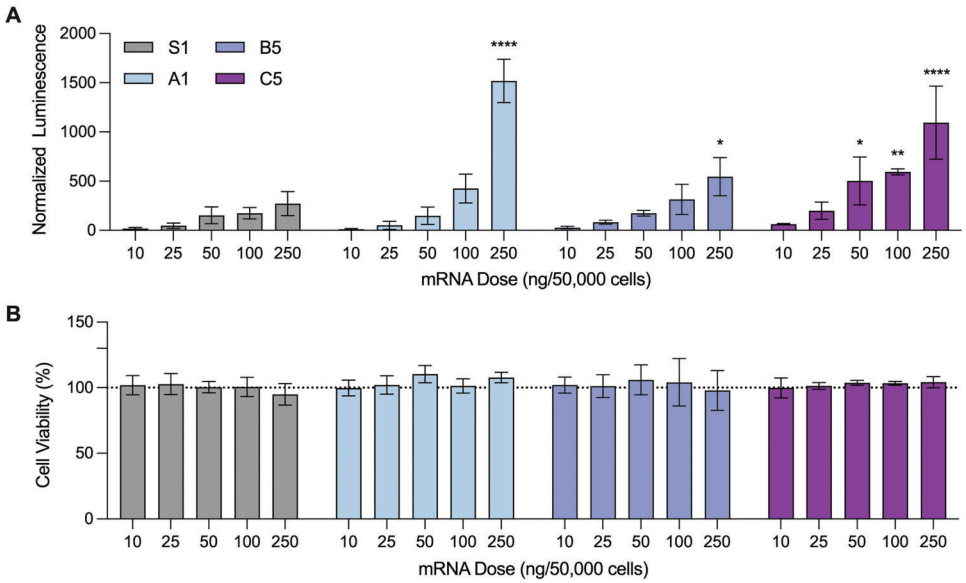

Figure 4. In vitro dose-response of top performing LNPs from libraries A, B, and C. A) Luciferase expression and B) cell viability of BeWo b30 cells 24 h after treatment with S1, A1, B5, or C5 LNPs. Cells were treated in a dose dependent manner at 10, 25, 50, 100, or 250 ng of luciferase mRNA per 50 000 cells. Luminescence and cell viability were quantified by normalizing to untreated cells (dashed line). Results are reported as mean ± standard deviation from $n = 3$ biological replicates. A two-way ANOVA with post hoc Student's t tests using the Holm–Šídák correction for multiple comparisons was used to compare the luciferase expression or cell viability across treatment groups and dosing amounts to LNP S1, $*p \leq 0.05$, $**p \leq 0.01$, $****p \leq 0.0001$.

2.4. Optimized LNP C5 Achieves Greater In Vivo Placental mRNA LNP Delivery Compared to LNP S1 in Pregnant Mice

On gestational day E16, pregnant mice were treated with PBS or LNPs S1, A1, and C5 at a dose of 0.6 mg kg^{-1} of luciferase mRNA via a tail vein injection. Mice were injected on gestational day E16 as this corresponds to the end of the second trimester in human pregnancy which is when many placental disorders are diagnosed.[21,46–48] 6 h after treatment, mice were injected with luciferin via an intraperitoneal injection, euthanized and the maternal organs, placentas and fetuses were removed for bioluminescence imaging with an in vivo imaging system (IVIS) (**Figure 5**A,C,E). Bioluminescence signal in each organ was measured and quantified through regions of interest (ROIs). In the maternal organs, bioluminescence signal was observed in the liver and the spleen for all LNP-treated mice (Figure 5A,B and Figure S3, Supporting Information). In the liver, LNP A1 exhibited greater mRNA delivery compared to LNP S1 while LNP C5 demonstrated reduced mRNA delivery compared to both LNPs A1 and S1. In the spleen, both LNPs A1 and C5 exhibited increased mRNA delivery compared to LNP S1, demonstrating the ability of these optimized LNPs to achieve improved extrahepatic delivery compared to the standard formulation.

Differences in the observed mRNA delivery to the maternal organs for each LNP formulation may be attributed to their excipient compositions. As previously mentioned, LNP S1 is formulated at a molar composition of 35% C12-494:16% DOPE:46.5% cholesterol:2.5% PEG. On the other hand, LNP A1 has increased amounts of C12-494 and DOPE and reduced levels of cholesterol and PEG, and LNP C5 has increased amounts of C12-494 and decreased amounts of cholesterol compared to LNP S1. LNP A1 is formulated with a molar composition of 49.2% C12-494:32.8% DOPE:16.4% cholesterol:1.6% PEG and LNP C5 has a molar composition of 51.4% C12-494:14% DOPE:32.7% Cholesterol:1.9% PEG.

Previously, DOPE has been shown to influence mRNA delivery to the liver compared to other phospholipids such as DSPC.[5,7,41,42] Thus, the increased DOPE content in LNP A1 may be driving increased mRNA delivery to the liver compared to the other formulations. The increase in splenic mRNA delivery from LNP S1 to A1 to C5, which also correlates with increasing molar amounts of C12-494, may be explained by the structure of the C12-494 ionizable lipid. Previous work published by our lab using the C12-494 lipid to formulate LNPs demonstrated increased mRNA delivery to the spleen than the liver in pregnant mice.[15] There, the authors hypothesized that the extrahepatic splenic mRNA delivery could be attributed to the lipid structure of C12-494, where the ether linkages impact the overall electronegativity of the lipid and potentially contribute to the observed splenic mRNA delivery.[15] Additionally, a prior study observed splenic mRNA delivery following intravenous injection with an ionizable lipid which also contained oxygen-containing linkages. The authors attributed the observed splenic mRNA delivery to the potential for these linkages to be degraded in the liver, but remain intact in the splenic environment, which facilitated mRNA delivery to the spleen.[10] Given these two previous findings, it is likely that the presence of ether linkages in our ionizable lipid is facilitating mRNA delivery to the spleen, which can be enhanced through increasing the molar content of the C12-494 ionizable lipid in our LNP formulations. However, more work is needed to elucidate the exact mechanisms behind shifts in biodistribution due to changes in LNP excipient molar ratios.

We then imaged the placentas and fetuses and quantified bioluminescence signal in each treatment group. Only LNP C5 significantly improved mRNA delivery to the placenta compared to LNP S1, consistent with our in vitro results where LNP

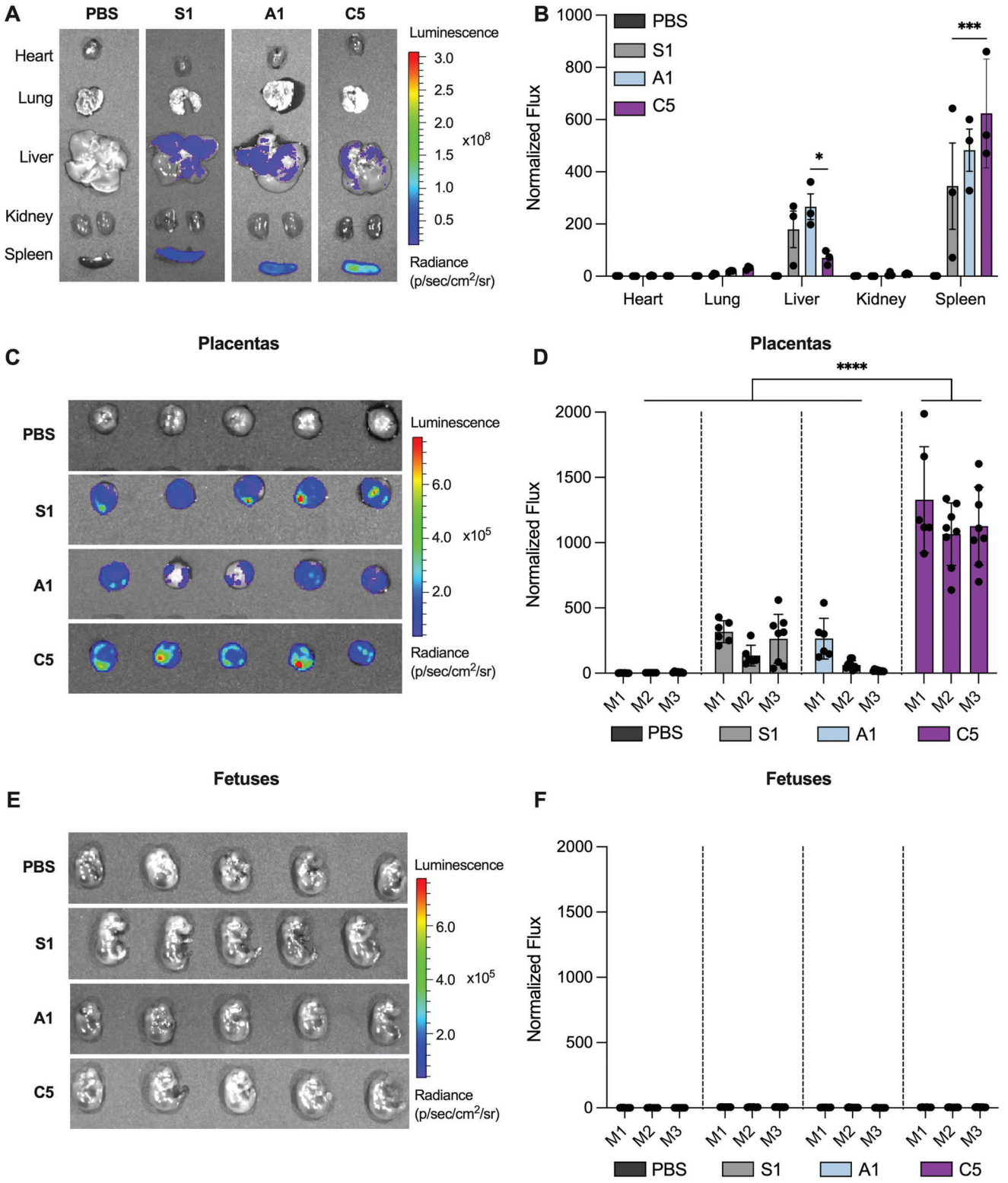

Figure 5. In vivo luciferase mRNA LNP delivery in pregnant mice to the maternal organs, placentas, and fetuses. A) IVIS images and B) quantification of luciferase mRNA LNP delivery to the maternal heart, lung, liver, kidney, and spleen in pregnant mice. Representative IVIS images are shown from the mouse with the normalized flux in the spleen closest to the mean. Normalized flux is reported as mean ± standard deviation from $n = 3$ biological replicates. A two-way ANOVA with post hoc Student's t tests using the Holm–Šídák correction for multiple comparisons was used to compare normalized flux across treatment groups and organs to LNP S1. $*p \leq 0.05$, $***p \leq 0.001$. C) IVIS images and D) quantification of luciferase mRNA LNP delivery to the placentas of pregnant mice. E) IVIS images and F) quantification of luciferase mRNA LNP delivery to the fetuses of pregnant mice. Representative

C5 was our lead candidate for mRNA delivery to trophoblasts (Figure 5C,D and Figure S4, Supporting Information). Despite having promising results in vitro, LNP A1 was unable to improve mRNA delivery to the placenta in vivo. Additionally, there was no bioluminescence signal in the fetuses for the LNP treated groups, suggesting that the LNPs remain in the placenta and do not enter fetal circulation, likely due to their >100 nm size which is expected to prevent placental transport (Figure 5E,F and Figure S4, Supporting Information).[15,17,18,48,49]

Organ specificity for each LNP formulation was also evaluated by summing the normalized luminescent flux from the maternal organs, placentas, and fetuses and calculating the percentage of total flux in each organ (Figure S5, Supporting Information). Across the treatment groups, LNP A1 had the greatest percentage of luminescent flux in the spleen and liver with only about 20% of the signal found in the placentas. LNP S1 also had strong signal in the liver and spleen, but had greater specificity to the placenta, with 38% of the total luminescent flux found in the placentas. However, our top LNP, C5, had the greatest specificity to the placenta with 65% of the total luminescent flux found in the placentas, 34% in the spleen, and less than 1% in the liver. The low specificity to the liver indicates the ability of LNP C5 to enhance extrahepatic delivery of mRNA, particularly to the placenta in pregnant mice. This is perhaps driven by both the increased molar content of the C12-494 ionizable lipid and the reduced molar content of DOPE compared to the S1 formulation. Overall, these findings were consistent with our in vitro results, where LNP C5 was identified as our lead candidate for mRNA delivery to trophoblasts. In vivo, LNP C5 was able to achieve significantly enhanced mRNA delivery to the placenta in comparison to both LNPs A1 and S1. These results further confirm the importance of optimizing the excipient molar ratios to enhance in vivo mRNA delivery to the placenta.

2.5. Evaluating Cellular-Specific In Vivo mRNA LNP Delivery to the Placenta Following Intravenous Administration of LNPs

To understand how differences in LNP excipient composition affect cell-specific in vivo mRNA delivery to the placenta, LNPs C5 and S1 were formulated with mCherry mRNA and administered intravenously in pregnant mice on gestational day E16 at a dose of 1 mg kg^{-1}. 12 h after treatment with LNPs or PBS, the mice were euthanized and their placentas were dissected, processed, and stained for immune cells ($CD45^+$), endothelial cells ($CD31^+$, $CD45^-$), and trophoblasts using cytokeratin-7 ($CK7^+$, $CD31^-$, $CD45^-$) (Figure S6, Supporting Information).[51–53]

Overall, both LNPs C5 and S1 were able to mediate in vivo mCherry mRNA delivery to placental immune cells, endothelial cells and trophoblasts compared to the PBS treated mice, however only LNP C5 was able to achieve significantly higher mCherry expression in endothelial cells and trophoblasts compared to the PBS group. Additionally, across all cell types, mice treated with LNP C5 had higher mean in vivo mCherry expression compared to mice treated with LNP S1. In immune cells, the LNP C5-treated mice had an mCherry positivity rate of 4.75% while the LNP S1-treated mice had an mCherry positivity rate of 3.85% and the PBS-treated mice exhibited 1.94% mCherry positivity (**Figure 6**A,B). Mice treated with LNPs C5 or S1 exhibited 4.78% or 3.85% of $mCherry^+$ endothelial cells, respectively, compared to the PBS treated mice which had 1.10% $mCherry^+$ endothelial cells (Figure 6C,D). Lastly, mice treated with LNP C5 had the highest percentage of $mCherry^+$ trophoblasts cells at 5.49% compared 4.51% and 1.65% $mCherry^+$ trophoblasts for the S1 and PBS treated mice, respectively (Figure 6E,F).

Taken together, these results suggest the ability of our optimized LNP C5 to improve in vivo mRNA delivery to three of the main cell types in the placenta: immune cells, endothelial cells, and trophoblasts. These three cell types are all target cells of interest due to their respective roles in the pathophysiology of several placental disorders and their ability to secrete proteins into the placental environment.[21,28,29] Furthermore, these results are consistent with our biodistribution findings where LNP C5 demonstrated improved mRNA delivery to the placenta compared to LNP S1. Despite seeing a greater improvement in placental luciferase mRNA delivery for LNP C5 in the biodistribution studies, LNP C5 achieved higher mean mCherry expression across immune cells, endothelial cells, and trophoblasts when compared to LNP S1. The magnitude of the difference in mRNA translation between the C5 and S1 treated mice in both experiments may be attributed to the difference in sensitivity between bioluminescence and fluorescence signals; bioluminescence signals are generally much more sensitive due to their high signal to noise ratio. Despite these differences, our optimized C5 LNP formulation demonstrated enhanced mRNA delivery to the entire placenta as well as to three of the individual cell types within the placental microenvironment.

3. Conclusion

In conclusion, we utilized orthogonal DOE to identify optimized LNP formulations for mRNA delivery to the placenta. Iterative LNP libraries with varied excipient molar ratios were screened in vitro in BeWo b30 cells, placental trophoblasts, for mRNA delivery and cytotoxicity. After screening, LNPs A1 and C5 were identified as lead candidates due to their ability to potently deliver mRNA in vitro with minimal cytotoxicity in comparison to the standard formulation, LNP S1. LNPs A1 and C5 were then validated in vivo for mRNA delivery to the placenta following intravenous administration in pregnant mice. There, only LNP C5 was able to achieve significantly higher mRNA delivery to the placenta compared to LNP S1, while also facilitating extrahepatic mRNA delivery to the spleen. Cell-specific delivery within the placental microenvironment was also used to evaluate LNP C5, where it achieved higher mean mCherry mRNA expression in trophoblasts, endothelial cells, and immune cells compared to LNP S1. Together, these results confirm that optimized

IVIS images of both the placentas and fetuses are shown from the mouse with the normalized flux in the placentas closest to the mean. Normalized flux is reported as mean ± standard deviation from $n = 3$ biological replicates (with $n = 6$–9 placentas and fetuses). Nested one-way ANOVAs with post hoc Student's t tests using the Holm–Šídák correction for multiple comparisons were used to compare normalized flux across treatment groups, $^{****}p \leq 0.0001$.

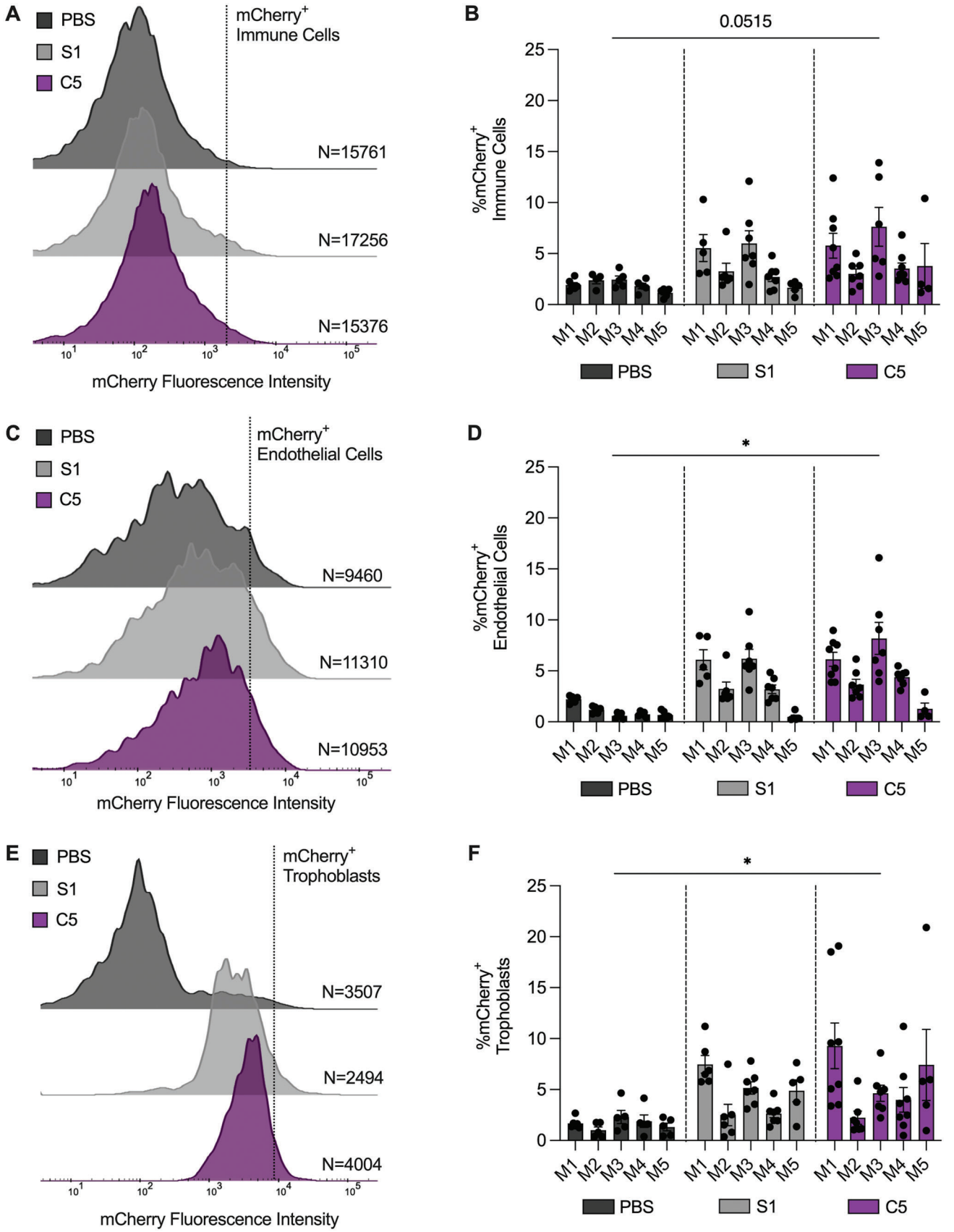

formulation of LNP C5 is a promising delivery platform for mRNA delivery to the placenta. Though future work should investigate the use of LNP C5 to deliver a therapeutically relevant mRNA cargo, such as VEGF of PlGF, in a murine model of placental insufficiency, the optimized C5 LNP formulation has demonstrated its ability to potently deliver mRNA to the placenta. Additionally, deeper investigations into the mechanisms behind enhanced mRNA delivery as a result of varied excipient composition will inform subsequent optimization of LNP formulations for placental mRNA delivery. We believe these optimization strategies can be applied to other LNP excipients and ionizable lipid structures to enhance nucleic acid delivery to the placenta and potentially beyond to other reproductive organs.

4. Experimental Section

Ionizable Lipid Synthesis: The C12-494 ionizable lipid was synthesized as previously described.[15] Briefly, the polyamine core 2-{2-[4-(2-{[2-(2 aminoethoxy)ethyl]amino}ethyl)piperazin-1-yl]ethoxy}ethan-1-amine (Enamine) was reacted with an excess of the epoxide tail 1,2-epoxydodecane (MilliporeSigma) under gentle stirring for 48 h at 80 °C. A Rotovapor R-300 rotary evaporator (Buchi) was used to dry the crude product and the lipid was resuspended in ethanol for ionizable lipid nanoparticle (LNP) formulation.

mRNA Synthesis: Luciferase mRNA with 5-methoxyuridine modifications for the in vitro assays and mCherry mRNA with N^1-methylpseudouridine modifications for the cell-specific flow cytometry experiments were purchased from Trilink Biotechnologies. For in vivo experiments, luciferase mRNA was synthesized with the pseudouridine modification using in vitro transcription as previously described.[54]

Lipid Nanoparticle Formulation and Characterization: LNPs were formulated at a weight ratio of 10:1 of ionizable lipid to mRNA.[5] For all formulations, the ionizable lipid C12-494, 1,2-dioleoyl-*sn*-glycero-3-phosphoethanolamine (DOPE, Avanti Polar Lipids), cholesterol (MilliporeSigma), and 1,2-dimyristoyl-*sn*-glycero-3-phosphoethanolamine-*N*-[methoxy(polyethylene glycol)-2000] (ammonium salt) (Lipid-PEG, Avanti Polar Lipids) were combined in an ethanol phase at various molar ratios specified in Table S1 (Supporting Information). 25 µg of mRNA was dissolved in 10 mM citric acid buffer (pH 3) to produce the aqueous phase. Syringe pumps were used to combine the ethanol and aqueous phases via chaotic mixing in a microfluidic device at a 1:3 volumetric ratio. Chaotic mixing was induced through herringbone features on the microfluidic device as previously described.[55] After synthesis, LNPs were dialyzed against 1X PBS for 2 h in cassettes with a 20 kDa molecular weight cut off and sterilized with 0.22 µm filters. LNPs were stored at 4 °C until use.

The mRNA concentration of each LNP formulation was measured via A260 absorbance on an Infinite 200 Pro plate reader (Tecan). Encapsulation efficiencies of each LNP formulation was measured using a Quant-iT-RiboGreen RNA assay (ThermoFisher Scientific). Briefly, each LNP formulation was diluted to ≈0.5 ng μL^{-1} in either 1X tris-EDTA (TE) buffer or TE buffer with 0.1% Triton X-100 (Millipore Sigma) and incubated for 20 min at room temperature to ensure particle lysis. LNPs in TE or Triton X-100 and mRNA standards were plated in triplicate in black 96-well plates and the RiboGreen reagent was added to each well. After 5 min of incubation at room temperature, the fluorescence intensity was read on a plate reader at an excitation wavelength of 480 nm and an emission wavelength of 520 nm. Encapsulation efficiencies were calculated as [(RNA content in TE buffer-RNA content in Triton X-100)/RNA content in Triton X-100]*100. mRNA concentration and encapsulation efficiencies are reported as mean ± standard deviation of $n = 3$ replicates.

Particle size as determined by dynamic light scattering (DLS) and zeta potential measurements were conducted using a Zetasizer Nano (Malvern Instruments). LNPs were diluted in either 1X PBS or water at pH 7 for either DLS measurements or zeta potential measurements, respectively. For each sample, three measurements with at least 10 runs were recorded. *Z*-average size, polydispersity index (PDI) and zeta potential are reported as mean ± standard deviation of $n = 3$ replicates.

The pK_a values of each LNP formulation were determined from a 6-(*p*-toluidinyl) naphthalene-2-sulfonic acid (TNS) assay. Briefly, buffered solutions of 150 mM sodium chloride, 20 mM sodium phosphate, 25 mM ammonium citrate, and 20 mM ammonium acetate were adjusted to a pH between 2 and 12 at 0.5 increments. LNPs were added to each pH adjusted solution and plated in triplicate in a black 96-well plate. TNS was added to each well for a final TNS concentration of 6 µM. The fluorescence intensity was measured on a plate reader at an excitation wavelength of 322 nm and an emission wavelength of 431 nm. The pK_a value of each LNP formulation was calculated as the pH at which the fluorescence intensity reached 50% of its maximum value, which represents 50% protonation.

In Vitro LNP-Mediated Luciferase mRNA Delivery to Trophoblast Cells: BeWo b30 cells were kindly provided by Dr. Dongeun Huh (University of Pennsylvania) with permission from Dr. Alan Schwartz (Washington University in St. Louis) and were cultured in Dulbecco's Modified Eagle Medium (Gibco) supplemented with 10% FBS (Gibco) and 1% penicillin-streptomycin (Gibco) and maintained at 37 °C and 5% CO_2. For all experiments, cells were plated at 50000 cells per well in 100 uL of media in 96-well plates and left to adhere overnight. To evaluate luciferase mRNA delivery by libraries A, B and C, the BeWo b30 cells were treated with LNPs at a dose of 50 ng of mRNA. 24 h after treatment with LNPs, media was removed from each well and the cells were resuspended in 50 µL of 1X lysis buffer (Promega) and 100 µL of luciferase assay substrate (Promega). After 10 min of incubation at room temperature, the luminescence signal was measured using a plate reader (Tecan). The luminescence signal for each treatment group was normalized to untreated wells and then divided by the average luminescence signal from the standard formulation (S1) treated wells. Relative luciferase expression is reported as mean ± standard deviation of $n = 3$ biological replicates (averaged from $n = 3$ technical replicates).

To quantify cytotoxicity of the cells following 24 h of treatment with LNPs, 100 µL of CellTiter-Glo (Promega) was added to each well. After 10 min of incubation at room temperature, the luminescence signal was measured using a plate reader and the luminescence signal for each treatment group was normalized to untreated wells. Percent cell viability is reported as mean ± standard deviation of $n = 3$ biological replicates (averaged from $n = 3$ technical replicates).

For the dose response experiment, BeWo b30 cells were seeded as described and dosed with either 10, 25, 50, 100, or 250 ng of mRNA. Both luciferase signal and cytotoxicity were measured as previously described and luminescence signal for each treatment group was normalized to untreated wells. Normalized luciferase expression is reported as mean ± standard deviation of $n = 3$ biological replicates (averaged from $n = 3$ technical replicates) and percent cell viability is reported as mean ± standard deviation of $n = 3$ biological replicates (averaged from $n = 3$ technical replicates).

Figure 6. Cell-specific in vivo mCherry mRNA LNP delivery to the placentas in pregnant mice. A) Representative histograms and B) quantification of percent $mCherry^+$ immune cells ($CD45^+$) in the placenta. C) Representative histograms and D) quantification of percent $mCherry^+$ endothelial cells ($CD31^+$ $CD45^-$) in the placenta. E) Representative histograms and F) quantification of percent $mCherry^+$ trophoblasts ($CK7^+$ $CD31^-$ $CD45^-$) in the placenta. Representative histograms with their respective cell counts are shown from the mouse with the value for percent $mCherry^+$ cells closest to the mean. Percent $mCherry^+$ cells are reported as mean ± SEM for $n = 5$ biological replicates (with $n = 4$–8 placentas). Nested one-way ANOVAs with post hoc Student's *t* tests using the Holm–Šídák correction for multiple comparisons were used to compare percent $mCherry^+$ cells across treatment groups, $^*p \leq 0.05$.

LNP-Mediated Luciferase mRNA Delivery in Pregnant Mice: All animal experiments were conducted in accordance with the guidelines and approval from the University of Pennsylvania's Institutional Animal Care and Use Committee (IACUC, protocol #806540). Time-dated pregnant C57BL/6 female mice (Jackson Laboratory) at gestational day E16 were tail-vein injected with LNPs containing luciferase mRNA or PBS at a dose of 0.6 mg mRNA kg^{-1} body mass. 6 h after injection, mice were injected via an intraperitoneal injection with *D*-luciferin potassium salt (Regis Technologies) at a dose of 150 mg of *D*-luciferin kg^{-1} of body mass. 10 min after *D*-luciferin administration, mice were euthanized with CO_2 and the heart, lung, liver, kidneys, spleen, and uterus were removed. The uterus was then dissected to remove the placentas and fetuses and all organs were imaged for luciferase signal with an in vivo imaging system (IVIS, PerkinElmer). Total luminescence flux was quantified using the Living Image software (PerkinElmer) where a rectangular region of interest (ROI) was placed around the organ, placenta or fetus of interest, and an equal sized ROI was placed in an area without any luminescent signal on the same image. Normalized flux was calculated by dividing the total flux from the organ, placenta or fetus ROI by the total flux of the corresponding background ROI. Normalized flux for the maternal organs is reported as mean ± standard deviation of $n = 3$ biological replicates. Normalized flux for the placentas and fetuses is reported as mean ± standard deviation of $n = 3$ biological replicates (with $n = 6$–9 placentas and fetuses).

Cell-Specific LNP-Mediated mCherry mRNA Delivery in the Placenta: Isolation of placental cells and subsequent flow cytometry was performed as previously described.[15] Briefly, time-dated pregnant C57BL/6 female mice at gestational day E16 were tail-vein injected with LNPs containing mCherry mRNA or PBS at a dose of 1 mg mRNA kg^{-1} body mass. 12 h after injection, the mice were euthanized with CO_2 and the uterus was removed and dissected to remove the placentas which were placed in 2 mL of deionized water on ice. The placentas and water were digested through 100 µm cell strainers (Thermo Fisher Scientific) to form cell suspensions. Each sample was then reacted with 200 µL of 10X DNase I buffer (New England BioLabs) and 20 µL of 2000 U mL^{-1} DNase I (New England BioLabs) for 30 min at room temperature. 2 mL of ACK lysis buffer (Thermo Fisher Scientific) was then added to each sample and centrifuged for 5 min at 300 *g*. After centrifugation, the supernatant was removed and the cells were resuspended in 0.5 mL of 1X PBS with 2 mM of EDTA and prepared for immunofluorescent staining.

First, 0.5 µL of TruStain FcX PLUS (anti-mouse CD16/32) (Biolegend) was added to the cells for 10 min on ice. Samples were then stained with 1.5 µL of FITC anti-mouse CD31 (Biolegend) and 3 µL of Brilliant Violet 421 anti-mouse CD45 antibody (Biolegend) for 30 min at 4 °C in the dark. Following incubation, each sample was rinsed once and resuspended in 100 µL of 1X PBS with 2 mM EDTA before fixation and permeabilization for intracellular staining using the Cyto-Fast Fix/Perm Buffer set (Biolegend). Samples were then stained intracellularly with 1 µL of Alexa Fluor 700 anti-mouse cytokeratin 7 (Novus Biologicals).

Data were acquired using a BD LSR II flow cytometer equipped with violet, blue, green and red lasers. For each sample, at least 50 000 events within the singlet gate were collected. mCherry positivity was determined using fluorescence minus one controls and gating was performed as seen in the representative gating schematic (Figure S6, Supporting Information). mCherry positivity for the placental immune cells, endothelial cells or trophoblasts are reported as mean ± SEM for $n = 5$ biological replicates (with $n = 4$–8 placentas).

Statistical Analysis: All statistical analyses were performed using GraphPad Prism. For the experiments screening libraries A, B, and C for in vitro luciferase expression and cell viability, nested one-way ANOVA with post hoc Student's *t* tests using the Holm–Šídák correction for multiple comparisons were used to compare the results across treatment groups to LNP S1. For the experiments screening the top performing LNPs in a dose-response for in vitro luciferase expression and cell viability, a two-way ANOVA with post hoc Student's *t* tests using the Holm–Šídák correction for multiple comparisons was used to compare the results across treatment groups and dosing amounts to LNP S1. For in vivo luciferase expression in maternal organs following LNP delivery to pregnant mice, a two-way ANOVA with post hoc Student's *t* tests using the Holm–Šídák correction for multiple comparisons was used to compare the results across treatment groups and organs. For in vivo luciferase expression in placentas and fetuses following LNP delivery to pregnant mice, nested one-way ANOVA with post hoc Student's *t* tests using the Holm–Šídák correction for multiple comparisons were used to compare the results across treatment groups. For in vivo mCherry mRNA delivery to immune cells, endothelial cells and trophoblasts in the placenta, nested one-way ANOVA with post hoc Student's *t* tests using the Holm–Šídák correction for multiple comparisons were used to compare mCherry positivity across treatment groups. For all figures, statistical significance is denoted by $*p \leq 0.05$, $**p \leq 0.01$, $***p \leq 0.001$, and $****p \leq 0.0001$.

Supporting Information

Supporting Information is available from the Wiley Online Library or from the author.

Acknowledgements

Figures 1–3 were created in part with Biorender.com. M.J.M. acknowledges support from a US National Institutes of Health (NIH) Director's New Innovator Award (DP2 TR002776), a Burroughs Wellcome Fund Career Award at the Scientific Interface (CASI), a US National Science Foundation CAREER award (CBET-2145491), and additional funding from the National Institutes of Health (NCI R01 CA241661, NCI R37 CA244911, and NIDDK R01 DK123049). H.C.S., K.L.S., H.C.G., A.G.H., and A.S.T. were supported by NSF Graduate Research Fellowships (Award 1845298).

Conflict of Interest

H.C.S., K.L.S. and M.J.M. have a patent application filed by the Trustees of the University of Pennsylvania describing the placenta mRNA lipid nanoparticle technology in this manuscript. All other authors declare they have no competing interests.

Data Availability Statement

The data that support the findings of this study are available from the corresponding author upon reasonable request.

Keywords

lipid nanoparticles, mRNA, placenta, pregnancy, women's health

Received: April 27, 2023
Revised: July 5, 2023
Published online: August 3, 2023

[1] X. Han, M. J. Mitchell, G. Nie, *Matter* **2020**, *3*, 1948.
[2] K. L. Swingle, A. G. Hamilton, M. J. Mitchell, *Trends Mol. Med.* **2021**, *27*, 616.
[3] K. A. Hajj, K. A. Whitehead, *Nat. Rev. Mater.* **2017**, *2*, 17056.
[4] X. Hou, T. Zaks, R. Langer, Y. Dong, *Nat. Rev. Mater.* **2021**, *6*, 1078.
[5] K. J. Kauffman, J. R. Dorkin, J. H. Yang, M. W. Heartlein, F. DeRosa, F. F. Mir, O. S. Fenton, D. G. Anderson, *Nano Lett.* **2015**, *15*, 7300.
[6] B. Li, X. Luo, B. Deng, J. Wang, D. W. McComb, Y. Shi, K. M. L. Gaensler, X. Tan, A. L. Dunn, B. A. Kerlin, Y. Dong, *Nano Lett.* **2015**, *15*, 8099.

[7] Q. Cheng, T. Wei, L. Farbiak, L. T. Johnson, S. A. Dilliard, D. J. Siegwart, *Nat. Nanotechnol.* **2020**, *15*, 313.
[8] K. A. Hajj, J. R. Melamed, N. Chaudhary, N. G. Lamson, R. L. Ball, S. S. Yerneni, K. A. Whitehead, *Nano Lett.* **2020**, *20*, 5167.
[9] M. A. Oberli, A. M. Reichmuth, J. R. Dorkin, M. J. Mitchell, O. S. Fenton, A. Jaklenec, D. G. Anderson, R. Langer, D. Blankschtein, *Nano Lett.* **2017**, *17*, 1326.
[10] O. S. Fenton, K. J. Kauffman, J. C. Kaczmarek, R. L. McClellan, S. Jhunjhunwala, M. W. Tibbitt, M. D. Zeng, E. A. Appel, J. R. Dorkin, F. F. Mir, J. H. Yang, M. A. Oberli, M. W. Heartlein, F. DeRosa, R. Langer, D. G. Anderson, *Adv. Mater.* **2017**, *29*, 1606944.
[11] P. S. Kowalski, A. Rudra, L. Miao, D. G. Anderson, *Mol. Ther.* **2019**, *27*, 710.
[12] M. M. Billingsley, N. Singh, P. Ravikumar, R. Zhang, C. H. June, M. J. Mitchell, *Nano Lett.* **2020**, *20*, 1578.
[13] F. P. Polack, S. J. Thomas, N. Kitchin, J. Absalon, A. Gurtman, S. Lockhart, J. L. Perez, G. Pérez Marc, E. D. Moreira, C. Zerbini, R. Bailey, K. A. Swanson, S. Roychoudhury, K. Koury, P. Li, W. V. Kalina, D. Cooper, R. W. Frenck, L. L. Hammitt, Ö. Türeci, H. Nell, A. Schaefer, S. Ünal, D. B. Tresnan, S. Mather, P. R. Dormitzer, U. Şahin, K. U. Jansen, W. C. Gruber, *N. Engl. J. Med.* **2020**, *383*, 2603.
[14] L. R. Baden, H. M. El Sahly, B. Essink, K. Kotloff, S. Frey, R. Novak, D. Diemert, S. A. Spector, N. Rouphael, C. B. Creech, J. McGettigan, S. Khetan, N. Segall, J. Solis, A. Brosz, C. Fierro, H. Schwartz, K. Neuzil, L. Corey, P. Gilbert, H. Janes, D. Follmann, M. Marovich, J. Mascola, L. Polakowski, J. Ledgerwood, B. S. Graham, H. Bennett, R. Pajon, C. Knightly, et al., *N. Engl. J. Med.* **2021**, *384*, 403.
[15] K. L. Swingle, H. C. Safford, H. C. Geisler, A. G. Hamilton, A. S. Thatte, M. M. Billingsley, R. A. Joseph, K. Mrksich, M. S. Padilla, A. A. Ghalsasi, M.-G. Alameh, D. Weissman, M. J. Mitchell, *J. Am. Chem. Soc.* **2023**, *145*, 4691.
[16] R. E. Young, K. M. Nelson, S. I. Hofbauer, T. Vijayakumar, M.-G. Alameh, D. Weissman, C. Papachristou, J. P. Gleghorn, R. S. Riley, Lipid Nanoparticle Composition Drives MRNA Delivery to the Placenta, Bioengineering, **2022**.
[17] N. Chaudhary, A. N. Newby, M. L. Arral, S. S. Yerneni, S. T. LoPresti, R. Doerfler, D. M. Strelkova Petersen, B. Fox, T. Coon, A. Malaney, Y. Sadovsky, K. A. Whitehead, Lipid Nanoparticle Structure and Delivery Route during Pregnancy Dictates MRNA Potency, Immunogenicity, and Health in the Mother and Offspring, Bioengineering, **2023**.
[18] C. G. Figueroa-Espada, S. Hofbauer, M. J. Mitchell, R. S. Riley, *Adv. Drug Delivery Rev.* **2020**, *160*, 244.
[19] N. M. Gude, C. T. Roberts, B. Kalionis, R. G. King, *Thromb. Res.* **2004**, *114*, 397.
[20] S. Al-Enazy, S. Ali, N. Albekairi, M. El-Tawil, E. Rytting, *Adv. Drug Delivery Rev.* **2017**, *116*, 63.
[21] E. Dimitriadis, D. L. Rolnik, W. Zhou, G. Estrada-Gutierrez, K. Koga, R. P. V. Francisco, C. Whitehead, J. Hyett, F. da Silva Costa, K. Nicolaides, E. Menkhorst, *Nat. Rev. Dis. Primers* **2023**, *9*, 8.
[22] A. Malhotra, B. J. Allison, M. Castillo-Melendez, G. Jenkin, G. R. Polglase, S. L. Miller, *Front. Endocrinol.* **2019**, *10*, 55.
[23] L. C. Chappell, C. A. Cluver, J. Kingdom, S. Tong, *Lancet* **2021**, *398*, 341.
[24] K. L. Swingle, A. S. Ricciardi, W. H. Peranteau, M. J. Mitchell, *Nat. Rev. Bioeng.* **2023**, *1*, 408.
[25] H. C. Geisler, H. C. Safford, M. J. Mitchell, *Small. Portico.* **2023**, https://doi.org/10.1002/smll.202300852.
[26] L. Woods, V. Perez-Garcia, M. Hemberger, *Front. Endocrinol.* **2018**, *9*, 570.
[27] M. Hemberger, C. W. Hanna, W. Dean, *Nat. Rev. Genet.* **2020**, *21*, 27.
[28] M. Knöfler, S. Haider, L. Saleh, J. Pollheimer, T. K. J. B. Gamage, J. James, *Cell. Mol. Life Sci.* **2019**, *76*, 3479.
[29] A. Umapathy, L. W. Chamley, J. L. James, *Angiogenesis* **2020**, *23*, 105.
[30] I. Aneman, D. Pienaar, S. Suvakov, T. P. Simic, V. D. Garovic, L. McClements, *Front. Immunol.* **2020**, *11*, 1864.
[31] K. L. Swingle, M. M. Billingsley, S. K. Bose, B. White, R. Palanki, A. Dave, S. K. Patel, N. Gong, A. G. Hamilton, M.-G. Alameh, D. Weissman, W. H. Peranteau, M. J. Mitchell, *J. Controlled Release* **2022**, *341*, 616.
[32] M. M. Billingsley, A. G. Hamilton, D. Mai, S. K. Patel, K. L. Swingle, N. C. Sheppard, C. H. June, M. J. Mitchell, *Nano Lett.* **2022**, *22*, 533.
[33] Q. Cheng, T. Wei, Y. Jia, L. Farbiak, K. Zhou, S. Zhang, Y. Wei, H. Zhu, D. J. Siegwart, *Adv. Mater.* **2018**, *30*, 1805308.
[34] K. J. Kauffman, M. J. Webber, D. G. Anderson, *J. Controlled Release* **2016**, *240*, 227.
[35] Y. Granot, D. Peer, *Semin. Immunol.* **2017**, *34*, 68.
[36] V. Kumar, J. Qin, Y. Jiang, R. G. Duncan, B. Brigham, S. Fishman, J. K. Nair, A. Akinc, S. A. Barros, P. V. Kasperkovitz, *Mol. Ther. – Nucleic Acids* **2014**, *3*, e210.
[37] A. Abdelkhaliq, M. van der Zande, R. J. B. Peters, H. Bouwmeester, *Part. Fibre Toxicol.* **2020**, *17*, 11.
[38] H. Tang, Z. Jiang, H. He, X. Li, H. Hu, N. Zhang, Y. Dai, Z. Zhou, *Int. J. Nanomed.* **2018**, *13*, 4073.
[39] L. Aengenheister, K. Keevend, C. Muoth, R. Schönenberger, L. Diener, P. Wick, T. Buerki-Thurnherr, *Sci. Rep.* **2018**, *8*, 5388.
[40] H. Li, B. van Ravenzwaay, I. M. C. M. Rietjens, J. Louisse, *Arch. Toxicol.* **2013**, *87*, 1661.
[41] R. Zhang, R. El-Mayta, T. J. Murdoch, C. C. Warzecha, M. M. Billingsley, S. J. Shepherd, N. Gong, L. Wang, J. M. Wilson, D. Lee, M. J. Mitchell, *Biomater. Sci.* **2021**, *9*, 1449.
[42] S. T. LoPresti, M. L. Arral, N. Chaudhary, K. A. Whitehead, *J. Controlled Release* **2022**, *345*, 819.
[43] Y. Fang, J. Xue, S. Gao, A. Lu, D. Yang, H. Jiang, Y. He, K. Shi, *Drug Delivery* **2017**, *24*, 22.
[44] D. Pozzi, V. Colapicchioni, G. Caracciolo, S. Piovesana, A. L. Capriotti, S. Palchetti, S. De Grossi, A. Riccioli, H. Amenitsch, A. Laganà, *Nanoscale* **2014**, *6*, 2782.
[45] C. Hald Albertsen, J. A. Kulkarni, D. Witzigmann, M. Lind, K. Petersson, J. B. Simonsen, *Adv. Drug Delivery Rev.* **2022**, *188*, 114416.
[46] C. A. Waker, M. R. Kaufman, T. L. Brown, *Front. Physiol.* **2021**, *12*, 681632.
[47] S. A. Elmore, R. Z. Cochran, B. Bolon, B. Lubeck, B. Mahler, D. Sabio, J. M. Ward, *Toxicol. Pathol.* **2022**, *50*, 60.
[48] S. E. Ander, M. S. Diamond, C. B. Coyne, *Sci. Immunol.* **2019**, *4*, 6114.
[49] M. Semmler-Behnke, J. Lipka, A. Wenk, S. Hirn, M. Schäffler, F. Tian, G. Schmid, G. Oberdörster, W. G. Kreyling, *Part. Fibre Toxicol.* **2014**, *11*, 33.
[50] P. K. Myllynen, M. J. Loughran, C. V. Howard, R. Sormunen, A. A. Walsh, K. H. Vähäkangas, *Reprod. Toxicol.* **2008**, *26*, 130.
[51] S. T. Kim, T. L. Adair-Kirk, R. M. Senior, J. H. Miner, *PLoS One* **2012**, *7*, e41348.
[52] J. Maldonado-Estrada, E. Menu, P. Roques, F. Barré-Sinoussi, G. Chaouat, *J. Immunol. Methods* **2004**, *286*, 21.
[53] C. Q. E. Lee, L. Gardner, M. Turco, N. Zhao, M. J. Murray, N. Coleman, J. Rossant, M. Hemberger, A. Moffett, *Stem Cell Rep.* **2016**, *6*, 257.
[54] N. Pardi, S. Tuyishime, H. Muramatsu, K. Kariko, B. L. Mui, Y. K. Tam, T. D. Madden, M. J. Hope, D. Weissman, *J. Controlled Release* **2015**, *217*, 345.
[55] D. Chen, K. T. Love, Y. Chen, A. A. Eltoukhy, C. Kastrup, G. Sahay, A. Jeon, Y. Dong, K. A. Whitehead, D. G. Anderson, *J. Am. Chem. Soc.* **2012**, *134*, 6948.